Tolerogenic IL-10-engineered dendritic cell-based therapy to restore antigen-specific tolerance in T cell mediated diseases

Laura Passeri [a], Grazia Andolfi [a], Virginia Bassi [a,b], Fabio Russo [a], Giorgia Giacomini [a], Cecilia Laudisa [a,1], Ilaria Marrocco [a,1], Luca Cesana [a,1], Marina Di Stefano [c], Lorella Fanti [d], Paola Sgaramella [c], Serena Vitale [e], Chiara Ziparo [f], Renata Auricchio [g], Graziano Barera [c], Giovanni Di Nardo [f], Riccardo Troncone [g], Carmen Gianfrani [e], Andrea Annoni [a], Laura Passerini [a,2], Silvia Gregori [a,*,2]

[a] Mechanisms of Peripheral Tolerance Unit, San Raffaele Telethon Institute for Gene Therapy (SR-Tiget), IRCCS San Raffaele Scientific Institute, Via Olgettina 60, 20132, Milan, Italy
[b] University of Rome Tor Vergata, Via Cracovia 50, 00133, Rome, Italy
[c] Department of Paediatrics, IRCCS San Raffaele Scientific Institute, Via Olgettina 60, 20132, Milan, Italy
[d] Gastroenterology and Gastrointestinal Endoscopy Unit, IRCCS San Raffaele Scientific Institute, Via Olgettina 60, 20132, Milan, Italy
[e] Institute of Biochemistry and Cell Biology, CNR, via P.Castellino 11, 80131, Naples, Italy
[f] NESMOS Department, School of Medicine and Psychology, Sapienza University of Rome, Sant'Andrea University Hospital, Via di Grottarossa 1035, 00189, Rome, Italy
[g] European Laboratory for the Investigation of Food Induced Diseases (ELFID), Department of Translational Medical Science, Section of Pediatrics, Via Pansini 5, 80131, University Federico II, Naples, Italy

ARTICLE INFO

ABSTRACT

Tolerogenic dendritic cells play a critical role in promoting antigen-specific tolerance *via* dampening of T cell responses, induction of pathogenic T cell exhaustion and antigen-specific regulatory T cells. Here we efficiently generate tolerogenic dendritic cells by genetic engineering of monocytes with lentiviral vectors co-encoding for immunodominant antigen-derived peptides and IL-10. These transduced dendritic cells (designated $DC^{IL-10/Ag}$) secrete IL-10 and efficiently downregulate antigen-specific $CD4^+$ and $CD8^+$ T cell responses from healthy subjects and celiac disease patients *in vitro*. In addition, $DC^{IL-10/Ag}$ induce antigen-specific $CD49b^+LAG-3^+$ T cells, which display the T regulatory type 1 (Tr1) cell gene signature. Administration of $DC^{IL-10/Ag}$ resulted in the induction of antigen-specific Tr1 cells in chimeric transplanted mice and the prevention of type 1 diabetes in pre-clinical disease models. Subsequent transfer of these antigen-specific T cells completely prevented type 1 diabetes development. Collectively these data indicate that $DC^{IL-10/Ag}$ represent a platform to induce stable antigen-specific tolerance to control T-cell mediated diseases.

1. Introduction

Failure of one or more players involved in the mechanisms sustaining immune tolerance to self or non-harmful antigens (Ags) can cause unwanted immune responses, leading to the development of T cell mediated diseases, such as autoimmunity [] Add Ref 1 in the brachet [2]. Currently approved therapies for the management of patients with autoimmune diseases vary from administration of immunosuppressive drugs to supportive therapies, such as insulin supplementation for type 1 diabetes (T1D), or changes in the lifestyle, as for lifelong gluten-free-diet (GFD) for celiac disease (CD) patients [3,4]. Although current therapies control symptoms of the disease, they negatively impact the patients' quality of life and are not devoid of side effects [5,6]. Critically, these therapies must be given lifelong to partially compensate for organ dysfunction, but they do not treat the cause of the disease and therefore they are not curative. Thus, there is a significant unmet need for safe and

---

effective treatments for these diseases. Ideally, such therapies should be well-tolerated and target the cause of disease to reduce duration and frequency of treatment, as well as to limit side effects. In this regard, Ag-specific therapies that selectively target detrimental immune response against disease related Ags are promising approaches.

Dendritic cells (DC) play a critical role in promoting immunological tolerance [7] through various mechanisms, which include depletion of autoreactive T cells [8], expression of inhibitory molecules [9,10] and peripheral induction of regulatory T cells (Tregs) [11,12]. These observations led to exploring the use of DC rendered tolerogenic *in vitro* (tolDC) to permanently restore Ag-specific tolerance [7,13]. TolDC have been generated in various ways from human CD14$^+$ monocytes. These include the use of antisense oligodeoxyribonucleotides targeting co-stimulatory molecules [14], treatment with Dexamethasone [15], Vitamin D3 [16], Rapamycin [17], IL-10 (DC-10) [11] or GM-CSF [18]. These tolDC express low levels of costimulatory molecules, secrete immunosuppressive cytokines *in vitro* and induce Tregs, the final mediators of tolerance [1]. First-in-man-studies with *ex vivo*-generated tolDC for the treatment of autoimmune diseases showed the feasibility and safety of the approach [14,19–21], but considerable heterogeneity in efficacy outcomes were observed [13,14,19,20]. Despite these encouraging results, routine use of tolDC-based approaches in clinical practice for the cure of autoimmune diseases requires that the generation and optimal tolerance inducing capacity of these DC needs to be further improved. To achieve this goal, we used lentiviral vectors (LVs) encoding for both human (h)IL-10 and specific autoimmune disease associated peptides fused to the invariant chain (Ii) to transduce DC (DC$^{IL-10/Ag}$). These DC$^{IL-10/Ag}$ cells secrete supra-physiological levels of IL-10, down regulate pathogenic CD4$^+$ and CD8$^+$ T cell responses *in vitro* and induce Ag-specific type 1 T regulatory (Tr1) cells *in vivo*, preventing disease development in pre-clinical models of T1D. Our results demonstrate for the first time that DC$^{IL-10/Ag}$ have the potential to restore Ag-specific tolerance in T cell mediated pathological conditions, including autoimmunity, and pave the way for a clinical translation of the approach.

2. Materials and methods

2.1. Human samples

Human peripheral blood was obtained in accordance with Ethical Committee of San Raffaele Hospital (OSR) and written informed consent was received prior to participation to the study, according to the Declaration of Helsinki (Protocols TIGET09/TIGET12b). Peripheral blood mononuclear cells (PBMC) were isolated *via* density gradient centrifugation over Lymphoprep (Cedarlane); CD14$^+$ monocytes were isolated using CD14 MicroBeads (Miltenyi Biotech), according to the manufacturer's instructions. CD4$^+$/CD8$^+$ T cells were purified by using the human CD4$^+$/CD8$^+$ T-cell Isolation kits, respectively (Miltenyi Biotech), according to the manufacturer's instructions.

2.2. HLA-typing

HLA-A2$^+$ donors were selected by flow cytometry using anti-HLA-A2 mAb (Exbio, cloneBB7.2). For HLA-DQ screening, DNA was extracted from whole blood by QiAMP DNA-Blood-Mini kits (Qiagen), and presence of the alleles DQB1*0302 (HLADQ8), DQA1*05/DQB1*02 (HLADQ2.5), DQA1*0201/DQB1*02 (HLADQ2.2), DQA1*05/DQB1*0301 (HLADQ7) was investigated by PCR (EuGen Kit, Eurospital), following manufacturer's instructions.

2.3. Plasmids and vector production

Sequences encoding for peptides used to stimulate murine T cells (Ovalbumin (OVA)$_{242-353}$, OVA$_{315-353}$, InsulinB (InsB)$_{4-29}$, InsB$_{4-29R22E}$, 2.5Hybrid Peptide (HIP)) fused in frame to a sequence encoding for

murine Ii were synthetized (GeneArt) and subcloned into a pCCL plasmid under the control of the promoter of phosphoglycerate-kinase-1 (PGK1) [22]. To obtain the plasmid encoding for a designated Ag and IL-10, the sequences encoding for Ag and hIL-10 were subcloned into a bi-directional pCCL plasmid [23]. Sequences encoding for the human invariant chain isoform p33 (Iip33) harboring a specific Ag-derived peptide sequence within the CLIP site [InsB$_{4-29}$, α-Gliadin (α-Glia)$_{51-80}$, pre-pro insulin (PPI)$_{13-28}$ or tyrosine phosphatase-related islet antigen 2 (IA-2)$_{801-821}$] were subcloned into bi-directional pCCL plasmids [23] co-encoding for a truncated variant of nerve growth factor receptor (ΔLNGFR) or hIL-10. As control, plasmids encoding for the native Iip33 sequence were generated. For human CD8$^+$ T-cell stimulation, sequences encoding for Influenza A Matrix protein 1 (M1) and murine heat-stable antigen (mHSA/CD24) marker gene [24] or hIL-10 were subcloned into bi-directional pCCL plasmid, in sense and antisense, respectively. Vesicular Stomatitis Virus (VSV) pseudo-typed third-generation LVs were produced by transient four-plasmid co-transfection into 293 T cells and purified by ultracentrifugation, as described [22]. LV physical particles were measured by HIV-1-Gag p24-Ag immuno-capture assay (PerkinElmer), following manufacturer's instructions. For LV titration, 293 T cells were transduced with serial LV dilutions, followed by genomic DNA (gDNA) extraction and vector copy number (VCN) determination. LV infectivity was calculated as the ratio between infectious titer and physical particles.

2.4. Mice

All animal experiments were designed with a commitment to minimizing the number of mice and suffering, in accordance with the 3 R principle. The experimental protocols were approved by the Institutional Animal Care and Use Committee of the San Raffaele Scientific Institute (OSR) and by the Italian Ministry of Health (IACUC-702/1152/1155). C57Bl/6 ly45.1, C57Bl/6 ly45.2, Non-obese diabetic (NOD), and NOD.Cg-Prkdc(scid)Il2rg(tm1)Wjl (NSG) mice were purchased from Charles-River. OTI, OTII and BDC2.5 Vβ4$^+$ mice are maintained in the animal facility of OSR. BDC2.5-Vβ4$^+$ mice were screened by flow cytometry.

2.5. Human dendritic cell differentiation and transduction

PB-derived CD14$^+$ cells were cultured, at 10^6 cells/ml in Good Manifacturing Practice (GMP) Serum-free Dendritic-Cell Medium (CellGenix) supplemented with 100U/ml penicillin/streptomycin, 100 ng/ml rhGM-CSF plus 10 ng/ml rhIL-4 (Miltenyi Biotech) and 10 ng/ml rhIL-10 (CellGenix), only for IL-10-encoding LVs. Cells were pre-treated for 3–6 h with Vpx-VLPs and then transduced with LVs at MOI 5–20, as described [25]. Medium with rhGM-CSF and rhIL-4 was replenished on day 1/3. DC were collected at day 7.

2.6. Vector copy number determination

VCN was quantified by ddPCR using 10 ng of gDNA, primers and probes against 2-LTR regions of LV. Endogenous DNA amount was quantified by primers/probe set against the human telomerase gene. Droplet generation and quantification was performed by QX200 AutoDG and QX200 reader (Bio-Rad). Analysis was performed with QuantaSoft-Analysis-Pro Software (Bio-Rad). VCN was calculated upon normalization to telomerase gene.

2.7. Flow cytometry

Human DC were stained for 10min at RT with PromoFluor-840 Maleimide (Promocell) for dead cell exclusion, followed by 15min incubation at RT in staining buffer plus FcR-Blocking reagent (Miltenyi Biotech) containing combinations of the following mAbs: anti-CD11c cloneB-ly6, anti-CD14 cloneMφP9, anti-CD209 cloneDCN46, anti-

CD16 clone3G8, anti-CD86 clone2331(FUN-1), anti-CD141 clone1A4, anti-CD163 cloneGHI/61, anti-HLA-DR cloneG46-6 (all from BD Biosciences), anti-CD80 cloneMEM-233 (Invitrogen), anti-HLA-G clone87G (Exbio), anti-ILT4 clone287219 (R&D Systems), PD-L1 cloneMIH-1 (eBiosciences), anti-ΔNGFR cloneME20.4 and HLA_ABC cloneW6/32 (Biolegend). After incubation, cells were fixed in 1% Paraformaldehyde (PFA). For murine DC analysis, 5×10^4 cells were stained 15min at RT with the following mAbs mix diluted in staining buffer (PBS/2%FBS): anti-CD80 clone16-10A1, anti-CD86 cloneGL1, anti-CD40 clone3/23, anti-PDL-1 cloneMIH5 (all from BD Pharmingen), anti-CD11c cloneN418 (Invitrogen), anti-IA/IE cloneM5/114 (Biolegend), anti-CD83 cloneRE601 (Miltenyi Biotech), followed by fixation with 1%Paraformaldehyde (PFA) (Invitrogen). For proliferation or Treg differentiation, at the end of T/DC cocultures cells were stained for 10min at RT with LIVE/DEAD Fixable Dead-Cell-Stain (Invitrogen) or PromoFluor-840 Maleimide for dead cell exclusion, according to manufacturer's instructions, followed by incubation with mixtures of the following mAbs: i) human cells: anti-CD3 cloneHIT3a and anti-CD8 cloneSK1 (Biolegend), anti-CD4 cloneSK3/RPAT4, anti-CD25 clone2A3, anti-HLA-DR cloneG46-6 (all from BD Bioscience), anti-CD49b REA188, anti-LAG3 REA351 and anti-CD137 REA765 (Miltenyi Biotec), and anti-CD71 cloneOKT9 (eBioscience); ii) murine cells: anti-CD3 clone17A2, anti-CD4 cloneRM4-5, anti-CD8 clone53–7.3, anti-CD44 cloneIM-7, anti-CD25 clone7D4. For analysis of splenocytes from DC-treated mice, at EOE cells were incubated with the following mAbs: anti-CD45.1 cloneA20, anti-CD45.2 clone104, anti-CD3 clone17A2, anti-CD4 cloneRM4-5, anti-CD8 clone53–7.3, anti-CD44 cloneIM-7, anti-LAG-3 cloneC9B7WN, (all from BD Pharmingen), anti-CD49b cloneXMa2 (Biolegend) and anti-FoxP3 cloneFK-16s (eBioscience). Intranuclear Foxp3 staining was performed according to manufacturer's instructions (eBioscience). Samples were acquired using FACSCanto II or Symphony (BD Biosciences) or CytoFLEX-LX (Beckman Coulter) analyzers and data analyzed using FlowJo v10 software. Quadrant markers were set according to unstained controls. For Tr1 cell sorting, eFluor450-labelled T (DC$^{IL-10/Ins}$) or T(DC^{Ins}) were stained with the following mAbs: anti-CD3 cloneHIT3a, anti-CD4 cloneRPAT4, anti-CD49b REA188, anti-LAG-3 REA351 and sorted with BD-FACSAria (BD Biosciences) to obtain CD3$^+$CD4$^+$eFluor450$^-$CD49b$^+$LAG3$^+$ (Ag-specific Tr1) or CD3$^+$CD4$^+$efluor450$^-$ (Ag-specific non-Tr1).

2.8. Human T-DC cell co-cultures

Response of human CD4$^+$ T cells to DC^{Ins} and DC^{glia} and response of CD8$^+$ T cells to DC^{M1} was evaluated as follows: 15×10^4 T cells were cultured with DC at [1DC:10 T] ratio in X–VIVO 15 medium (Lonza), supplemented with 5% human serum and 100U/ml penicillin/streptomycin. After 6 days T-cell proliferation and/or expression of activation markers were evaluated by flow cytometry, as above described, and supernatant was collected for cytokine determination. For Tr1 cell induction, after 10 days DC-primed T cells were purified using CD3 microbeads (Miltenyi Biotech) and stained for flow cytometric analysis, after 3 days of resting.

2.9. Cytokine determination

Murine DC were plated at a density of 10^6 cells/ml and left unstimulated or stimulated with lipopolysaccharide (LPS) 200 ng/ml for 24 h, while human DC were plated at a density of $0,5 \times 10^6$ cells/ml and left unstimulated or stimulated with LPS 200 ng/ml plus IFN-γ 50 ng/ml (R&D Systems) for 48 h. Murine cytokines were quantified in culture supernatants by magnetic beads assay according to the manufacturer's instructions (Bio-Rad), while human cytokines were quantified by ELISA, as described [25].

2.10. RNA-sequencing

RNA-Seq was performed on sorted CD3$^+$CD4$^+$CD49b$^+$LAG3$^+$ Ag-specific (i.e., proliferation dye negative) Tr1 cells (T(DC$^{IL-10/Ins}$)) and Ag-specific non-Tr1 cells (T(DC^{Ins})). RNA was extracted with miRNeasy Kit (Qiagen), following manufacturer's instructions. After quality control by Qubit (ThermoFisher) and TapeStation (Agilent), libraries based on polyA-selection were built and sequenced by 2×150 Illumina Novaseq (Genewiz). RNA-Seq analyses are described in supplementary materials.

Bioinformatics analyses were implemented on Linux systems exploiting online available tools and in-house scripts based on bash, python (v3.8.6) and R (v3.5.0) languages. To assess the quality of the reads before and after trimming we used FastQC (v0.11.6) and MultiQC (v1.9) tool. Adapter ('CTGTCTCTTATA') and low-quality reads were removed using Trim Galore (v0.6.6) (www.bioinformatics.babraham.ac. uk/projects/trim_galore/). Only the reads with a quality score (Q) > 20 were used for further analyses. The resulting set of selected reads were aligned against the reference human genome GRChg38 using STAR (v2.7.6a) with standard input parameters [26]. Genes were annotated using GENCODEv35 gene annotations and the total counts of transcripts per gene were quantified with FeatureCounts (v2.0.1) [27]. After calculating the gene expression levels, a differential expression analysis between T(DC$^{IL-10/Ins}$) and T(DC^{Ins}) cells was performed using the DESeq2 R package [28]. The resulting P-values were adjusted using the Benjamini-Hochberg's approach. An adjusted P value (FDR) > 0.05 was defined as the cutoff for statistical significance. The genes with | log2FC|<1 and FDR<0.05 were considered as DEGs. The annotated genes were further analyzed by Gene set enrichment analyses (GSEA, htt ps://www.gsea-msigdb.org/gsea/index.jsp) [29], to assess whether a defined set of genes showed significant, concordant differences in terms of expression between two groups of a sample. Gene set permutation for each analysis was set as 1000 times. Gene sets with FDR < 0.25 were considered significantly enriched. The log2-normalized counts were used for visualization. Graphical output used ggplot2 and *ComplexHeatmap* in RStudio environment [30]. RNASeq data are deposited in the NCBI's Gene Expression Omnibus and are accessible through GEO Series accession number GSE199425.

2.11. IFNγ ELISPOT

2×10^5 CD8$^+$ T cells were plated in triplicates onto ELISPOT plates (Millipore) pre-coated with anti-IFNγ mAb (10 μg/ml, Mabtech clone1-D1K) in X–VIVO 15 medium, either alone or with 2×10^4 DC. After 42–48 h, IFNγ-producing cells were detected by biotin-conjugated anti-IFNγ mAb (1 μg/ml, Mabtech clone7-B6-1), followed by streptavidin-peroxidase (Roche) and reaction with 3-Amino-9-ethylcarbazole substrate set (BD Biosciences). Spots were counted by ImmunoSpot-S6-ultraV (Cellular Technology Limited)**.** Results were normalized to SFU/10^6 CD8$^+$ cells.

2.12. Murine dendritic cell differentiation and transduction

BM-derived DC were generated from BM progenitors of C57Bl/6 or NOD mice. Total BM cells were cultured at a density of 1×10^6/ml in IMDM (Corning) supplemented with 10%FBS, 100U/ml Penicillin/ Streptomycin (Euroclone) in the presence of murine granulocyte-macrophage-colony-stimulating factor (mGM-CSF, 25 ng/ml, R&D Systems) (hereafter complete IMDM medium). At day 2, transduction of DC with LVs at Multiplicity of Infection (MOI) 10 was performed. At day 3/ 5/8 complete IMDM medium was replenished. If necessary, DC were activated at day 8 with LPS 200 ng/ml (Invivogen) to obtain mDC. At day 9, DC were collected.

2.13. Murine T cell cultures

To obtain murine responder T cells mouse spleens were homogenized using frosted glass slides and filtered after red blood cell lysis to obtain single cell suspensions. CD3$^+$, CD4$^+$ and CD8$^+$ T cells were purified using Pan T, CD4$^+$ or CD8$^+$ T-cell Isolation kits (Miltenyi Biotech) from spleens from 6/8-week-old mice, according to the manufacturer's instructions. Murine T cells were then stained with eFluor670 cell-proliferation-dye (eBioscience), according to manufacturer's instructions. Murine T cells were cultured with DC at [1DC:10 T] ratio in complete IMDM for 2–5 days prior to evaluation of T-cell proliferation and expression of activation markers by flow cytometry, as above described.

2.14. Generation of chimeric mice

BM cells were isolated from femurs and tibias of C57Bl/6 ly5.1 of a donor mouse and mixed to BM of OTII transgenic mice (ly5.2) in the following ratio: 95% C57Bl/6 ly45.1/5% OTII, for a total of 2×10^6 cells/mouse. The C57Bl/6 ly5.1 recipient mice received total body irradiation and were reconstituted with the mixed cells by intravenous injection. Mice were monitored by physical parameters (weight/fur/hunch/skin lesions) and blood composition (hemocytometer) and considered fully reconstituted after 8 weeks.

2.15. Induced T1D models

To induce T1D in female NSG mice, 1×10^6 TCRtg BDC2.5 CD4$^+$ or 5×10^6 splenocytes from NOD diabetic mice were injected intraperitoneally or intravenously, respectively. DC were injected intraperitoneally according to the experimental plan (Fig. 3A). In second transfer model, 5×10^6 splenocytes from NSG mice transferred with NOD splenocytes and treated with DC were collected and ri-transferred to new NSG recipients 45 days after DC treatment. Blood glucose was measured every other day using a Breeze blood glucose monitoring system (Bayer). Diabetes development was determined by two consecutive measures of glycemia≥250 mg/dl.

2.16. Sepsis model

Female C56Bl/6 were injected intraperitoneally with DC (3×10^6 DC/mouse) and 3 days after 2.5 mg/kg of LPS (E. Coli 0111:B4, Sigma Aldrich) was injected intraperitoneally [31]. Plasma was collected after 4, 6 and 24 h post LPS injection and plasmatic cytokines were measured by Luminex Multiplex assay (BIORAD).

2.17. Statistics

For RNA-Seq, analysis procedure is described in supplementary materials. All other data were analyzed using GraphPad-Prism 8.0; i) for comparisons between two groups, non-parametric Mann-Whitney U or Wilcoxon signed-rank tests for unpaired or paired comparisons, respectively, were used; ii) for multiple dependent groups comparisons Friedman test with Benjamini-Hochberg FDR correction was applied. All results are presented as mean ± SEM, unless specified in the figure legend. Survival curves were analyzed with Log-rank (Mantel-Cox) test with Benjamini-Hochberg FDR correction for multiple groups comparisons. Response to LPS challenge was analyzed with two-way ANOVA test with Benjamini-Hochberg FDR correction for multiple groups comparisons. Differences were regarded as significant at p < 0.05. Inferential analyses were applied in presence of adequate sample sizes (n ≥ 5), otherwise only descriptive statistics are reported.

3. Results

3.1. Induction of pro-tolerogenic human Ag-specific DC by LV-mediated IL-10 gene transfer

We generated LV constructs encoding for human Ii isoform p33 (Iip33) harboring a specific peptide sequence within the class II invariant chain (CLIP) site [32–36] alone or in combination with hIL-10 (LV-IL-10) [23,37] (Fig. S1A). LV-Iip33Ag, LV-IL-10/Iip33Ag and control LV-Iip33CLIP were used to transduce peripheral blood (PB) CD14$^+$ monocytes during *in vitro* DC differentiation [25] to generate Ag-specific DC lacking or expressing hIL-10 (DC^{Ag} and DC$^{IL-10/Ag}$) or control DC (DC^{CLIP}) (Fig. S1B). As Ags we used known HLA class II-restricted peptides derived from T1D and pathogenic celiac disease (CD) Ags (Fig. S1A) [38].

As a first step, we engineered PB CD14$^+$ cells from HLA-DQ8$^+$ healthy subjects with LVs co-encoding for InsB$_{4-29}$ (including the HLA-DQ8-restricted epitope InsB$_{9-23}$) and hIL-10 or ΔNGFR (DC$^{IL-10/Ins}$ or DC^{Ins}, respectively). DC^{CLIP} were differentiated in parallel (Fig. S1). We achieved efficient transduction of DC precursors, as demonstrated by the (VCN), the expression of the marker gene ΔNGFR by control DC and sustained spontaneous IL-10 production by DC$^{IL-10/Ins}$ (Fig. S2).

LV-engineered monocytes efficiently differentiated into DC, as defined by DC-SIGN and HLA-DR expression (Fig. 1A). DC$^{IL-10/Ins}$ expressed significant lower amounts of CD86 compared to control DC, although their co-stimulatory potential was warranted by a significant higher expression of CD80 (Fig. 1A). DC$^{IL-10/Ins}$ displayed a significant increased expression of tolDC-associated markers CD14, CD141, CD163, ILT4 and HLA-G [11,39] compared to control DC (Fig. 1B).

Upon activation with LPS and IFNγ, DC$^{IL-10/Ins}$ showed a marked anti-inflammatory cytokine production profile, with a significant higher IL-10 release and a drastic decrease of IL-12 and TNFα production compared to control DC (Fig. 1C). In line with our previous report [25], upon ectopic expression of IL-10, IL-6 production was not suppressed in DC$^{IL-10/Ins}$ compared to control DC (Fig. 1C).

3.2. Human DC$^{IL-10/Ag}$ modulate Ag-specific CD4$^+$ T cell responses and promote bona fide Ag-specific Tr1 cells

We characterized the ability of human DC$^{IL-10/Ins}$ to present the encoded Ag and modulate autologous CD4$^+$ T cell responses by measuring T cell activation, proliferation, and phenotype. Despite the low frequency of Ins-specific CD4$^+$ T cells in PB of HLA-DQ8$^+$ healthy subjects, DC^{Ins} induced InsB-specific CD4$^+$ T cell activation and/or proliferation in 11 out of 14 donors tested (Fig. 2A). Interestingly, DC$^{IL-10/Ag}$ promoted the generation of InsB-specific CD4$^+$ T cells with significant lower CD25 expression and reduced proliferation compared to DC^{Ins} (Fig. 2A). In addition, stimulation of autologous T cells with DC$^{IL-10/Ins}$ for 10 days induced Ins-specific CD4$^+$ T cells that contained significant higher frequencies of CD49b$^+$LAG-3$^+$ Tr1 cells [40] compared to those obtained with T cells stimulated with DC^{Ins} (n = 10, Fig. 2B).

To confirm that DC$^{IL-10/Ins}$ induce *bona fide* Ins-specific Tr1 cells *in vitro*, we performed RNA sequencing (RNA-Seq) on sorted Ins-specific CD49b$^+$LAG-3$^+$ Tr1 cells, obtained after a 10-day culture of CD4$^+$ T cells with autologous DC$^{IL-10/Ins}$ [T(DC$^{IL-10/Ins}$) cells. As control, Ins-specific non-Tr1 cells [T(DC^{Ins})], obtained after culture of CD4$^+$ T cells with autologous DC^{Ins} and sorting of proliferated cells, were sequenced in parallel (n = 3). Differential gene expression analysis between T(DC$^{IL-10/Ins}$) and T(DC^{Ins}) cells was performed using the R/Bioconductor package DESeq2 [28]. Based on the cut-off criteria (FDR < 0.05 and log2FC > 1), 1014 genes out of 35346 resulted as differentially expressed genes (DEGs), including 487 upregulated and 527 downregulated (Fig. 2C and Table S1). Notably, genes found upregulated in T(DC$^{IL-10/Ins}$) cells included the conventional Tr1 markers LAG-3 and ITGA2 (CD49b) and several genes previously described in
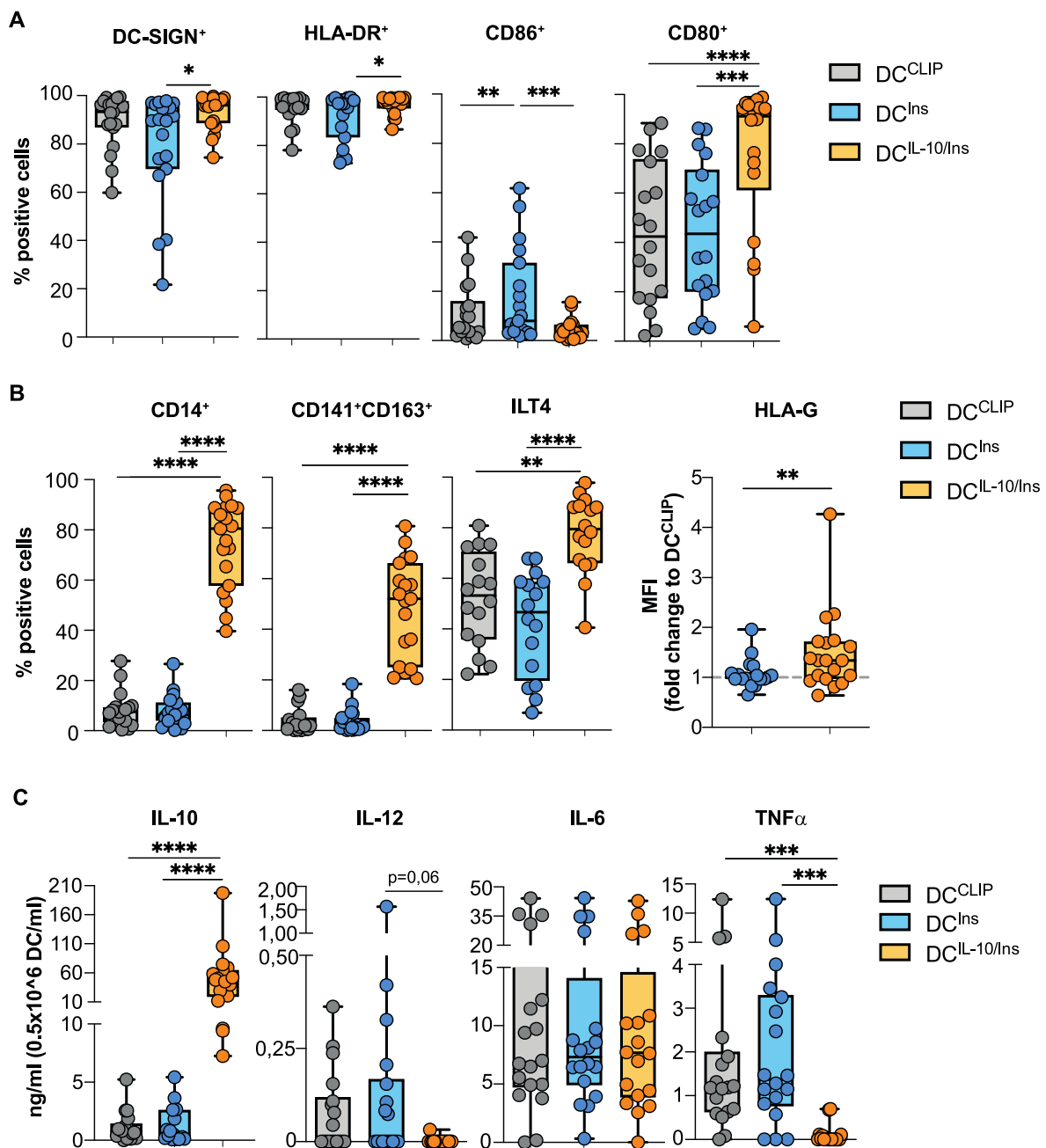
Fig. 1. DC$^{IL-10/Ins}$ are mature DC and display tolerogenic features. (A-B)
The expression of (A) differentiation/co-stimulation or (B) tolDC-associated markers on LV-transduced DC was assessed by flow cytometry. Percentage of positive cells is reported in the graphs; expression of HLA-G is reported as MFI normalized to donor-matched DC^{CLIP}, arbitrarily set to 1 (n = 16–19). (**C**) Concentration of IL-10, IL-12, TNFα and IL-6 in culture supernatant after 48 h stimulation with LPS/IFNγ was measured by ELISA. Box and whiskers (min to max) are presented, dots represent single donors (n = 17–18). *p < 0.05; **p < 0.01; ***p < 0.001; ****p < 0.0001, Friedman test with Benjamini-Hochberg correction for multiple comparisons, Wilcoxon signed-rank test for two-groups comparisons.

murine and human Tr1 cells, such as those required for cytotoxic function (IFNG, PRF1, GZMB, NKG7 and GZMA) [41], co-inhibitory molecules (PDCD1 - PD-1) [40,42], adhesion molecules (ITGAX, ITGA1) [40], and transcription factors (VDR and PRDM1) [43] (Fig. 2C). Genes commonly associated with thymic FOXP3$^+$ Tregs, such as FOXP3, IKZF2 and CCR7 were not upregulated (Fig. 2C) [44]. To verify molecular signatures enriched in T(DC$^{IL-10/Ins}$) cells, we applied Gene Set Enrichment Analysis (GSEA) [29], focusing on previously published Tr1 gene sets [40,43] (Tables S2–S3). T(DC$^{IL-10/Ins}$) cells were enriched for signatures of resting and TCR-stimulated Tr1 cell clones [40], and of the

T-allo10 cell product [43] (Fig. 2D, Tables S2–S3). Specifically, the upregulated genes included in the gene sets were significantly enriched in T(DC$^{IL-10/Ins}$) cells, while the downregulated genes were significantly enriched in T(DC^{Ins}) cells. Our analyses confirm that upon stimulation with DC$^{IL-10/Ins}$ Ins-responsive CD4$^+$ T cells acquire the archetypal Tr1 molecular signature.

In conclusion, DC engineered with LV co-encoding for InsB$_{4-29}$ and hIL-10 (DC$^{IL-10/Ins}$) tolDC modulate Ins-specific CD4$^+$ T cell responses and promote the differentiation of Ins-specific *bona fide* Tr1 cells *in vitro* in subjects carrying HLA-Q8 and autoreactive T cell clones.
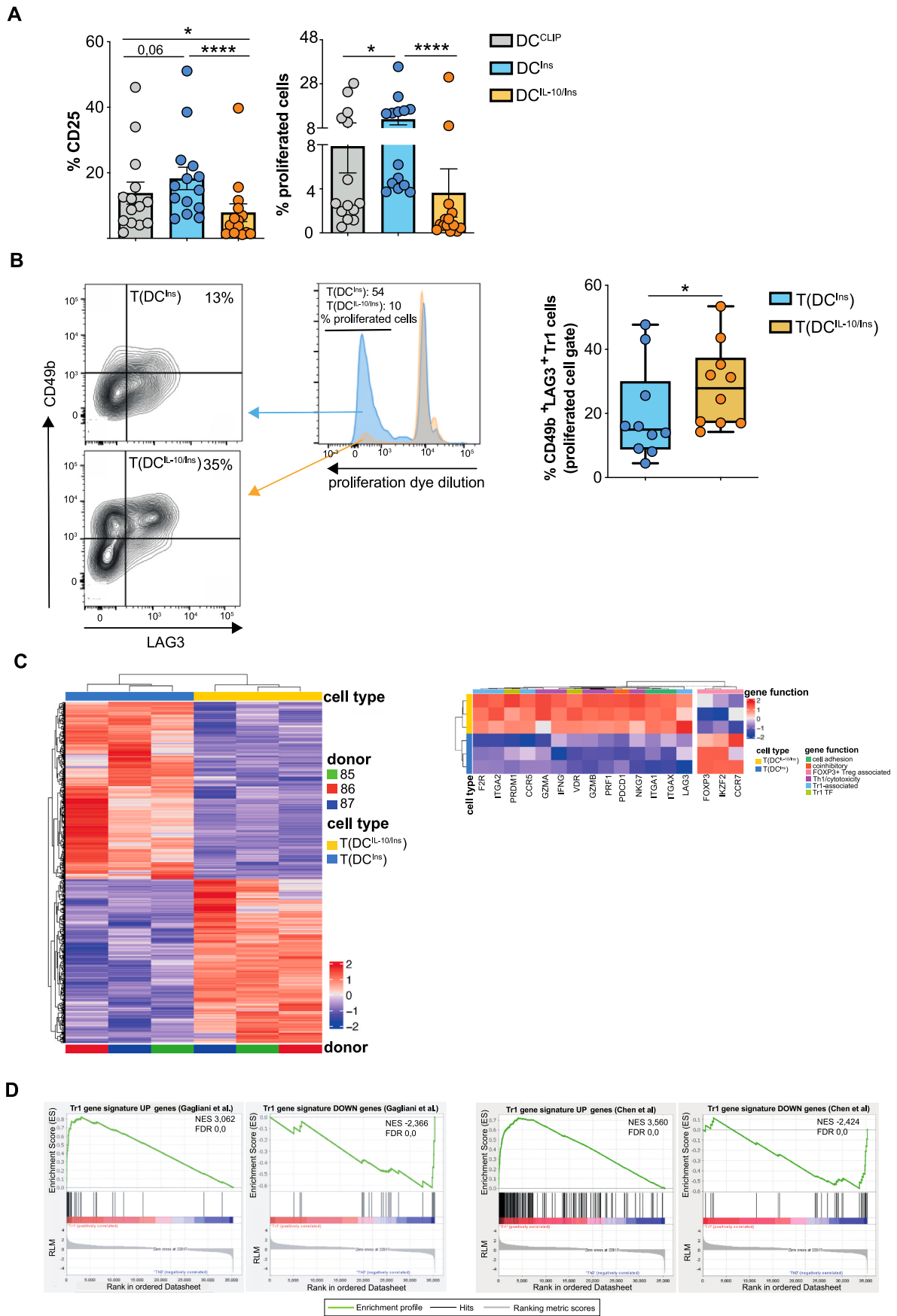
(caption on next page)

Fig. 2. Human DC$^{IL-10/Ag}$ modulate Ag-specific CD4$^+$ T cell responses and promote Ag-specific Tr1 cells. (A-B) LV-Iip33-CLIP (DC^{CLIP}), LV-Iip33-Ins$_{4-29}$ (DC^{Ins}) or LV-IL-10/Iip33-Ins$_{4-29}$ (DC$^{IL-10/Ins}$) transduced DC were cultured with proliferation-dye-labelled autologous CD4$^+$ T cells. (A) The frequency of CD25$^+$ T cells and of proliferated cells were measured by flow cytometry at day 6. Bars represent mean ± SEM and dots represent single donors (n = 14). *: p < 0.05, ****: p < 0.0001, Friedman test with Benjamini-Hochberg correction for multiple comparisons. (B) After 10 days T(DC^{Ins}) and T (DC$^{IL-10/Ins}$) cells were stained to detect Tr1 cells. Flow panels display the gating strategy used for analysis of a representative donor. The graph reports the frequency of CD49b$^+$LAG3$^+$ Tr1 cells within the proliferated (efluor-diluted) CD4$^+$ T cells. Box and whiskers (min to max) are presented, dots represent single donors (n = 10). *: p < 0.05, Wilcoxon signed-rank test. (C) T(DC$^{IL-10/Ins}$) cells were obtained after autologous CD4-DC$^{IL-10/Ins}$ co-culture from 3 HLA-DQ8$^+$ healthy subjects upon sorting of efluor-diluted T cells CD49b$^+$LAG-3$^+$. As control, efluor-diluted T cells were sorted in parallel from T-DC^{Ins} co-cultures (T(DC^{Ins}) cells). The upper heatmap shows DEGs between T(DC$^{IL-10/Ins}$) and T(DC^{Ins}) cells (FDR <0.05, |log2FC|>1). The lower heatmap depicts the expression of selected DEGs with function group as annotation. (D) GSEA was used to compare T(DC$^{IL-10/Ins}$) cells *vs* previously reported Tr1 gene-sets. Enrichment plots are shown; upper plots refer to Gagliani et al. [40], lower plots to Chen et al. [43]. RLM: ranked list metric; NES: normalized enrichment score; FDR: false discovery rate.
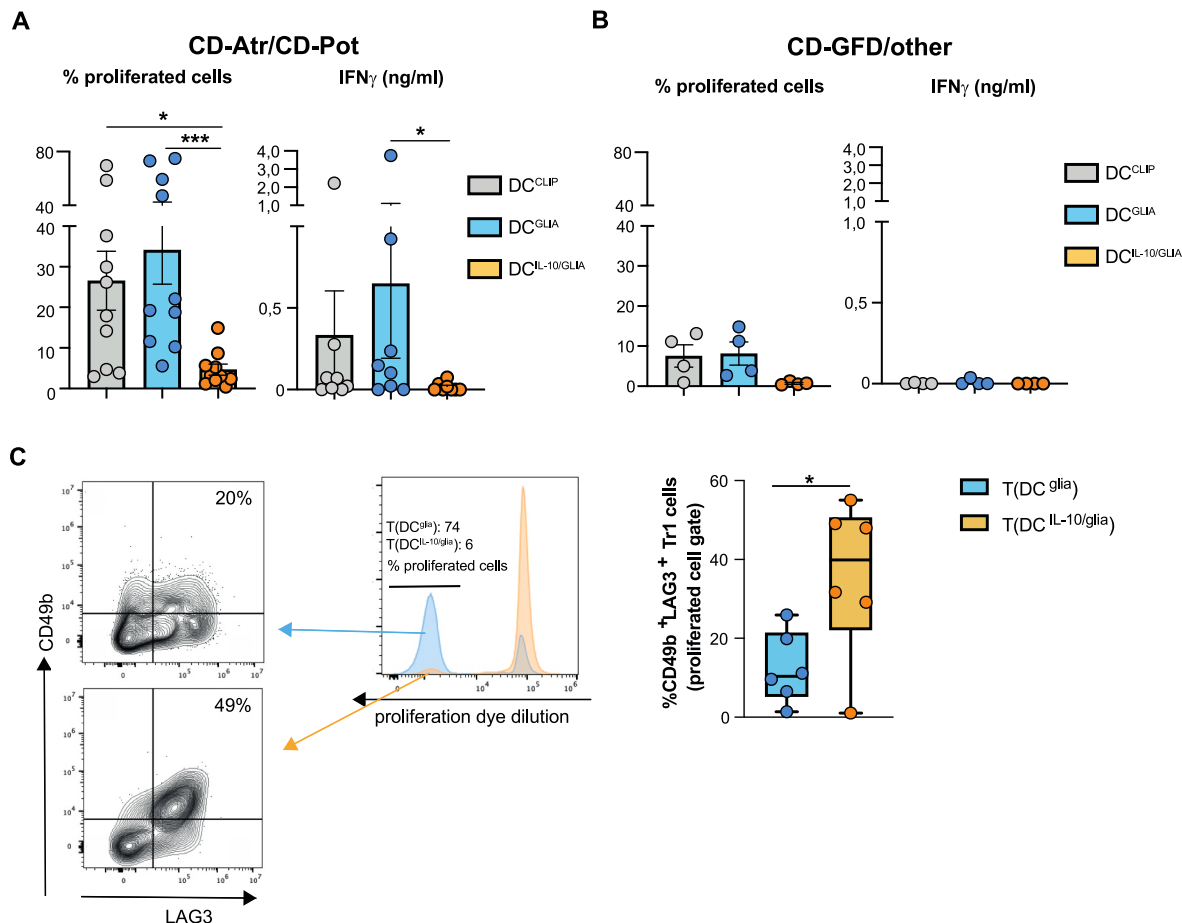
Fig. 3. DC$^{IL-10/glia}$ modulate gliadin-specific CD4$^+$ T cell responses of celiac disease patients. (A and B) LV-Iip33-CLIP (DC^{CLIP}), LV-Iip33-glia$_{51-80}$ (DC^{glia}) or LV-IL-10/Iip33-glia$_{51-80}$ (DC$^{IL-10/glia}$) transduced DC were cultured with proliferation-dye-labelled autologous CD4$^+$ T cells. After 6 days the percentage of proliferated cells was measured by flow cytometry. The concentration of IFNγ released in culture supernatant was measured by ELISA. Graphs in (A) report results from CD patients with atrophic mucosa (CD-Atr) or low Marsh score (CD-Pot), not undergoing GFD (n = 8–9). Graphs in (B) report results from CD patients on GFD (CD-GFD) and subjects with histology disproving CD diagnosis (other) (n = 4). Bars represent mean ± SEM and dots represent single donors. *: p < 0.05, ***: p < 0.001, Friedman test with Benjamini-Hochberg correction for multiple comparisons. (C) The frequency of CD49b$^+$LAG3$^+$ Tr1 cells within the proliferated (efluor-diluted) CD4$^+$ T cells was measured after autologous CD4$^+$ T/DC culture. Box and whiskers (min to max) are presented, dots represent single patients (n = 6). Flow panels display the gating strategy used for analysis. *p < 0.05, Wilcoxon signed-rank test.

3.3. Human DC$^{IL-10/Ag}$ modulate Ag-specific CD8$^+$ T cell responses

To characterize the ability of DC$^{IL-10/Ag}$ to present the encoded Ag in the context of MHC class I molecules and modulate CD8$^+$ T cell responses, a set of LVs encoding for known T1D-related HLA-A2-restricted epitopes (PPI$_{15-24}$, InsB$_{10-18}$, and IA-2$_{806-814}$) embedded in Iip33 sequence were generated [45–47] (Fig. S1). We engineered DC from HLA-A2$^+$ healthy subjects and tested their ability to stimulate autologous Ag-specific CD8$^+$ T cells *in vitro*. Unfortunately, CD8$^+$ T cell responses were barely detectable in all donors tested (n = 9) in terms of proliferation and IFNγ production (Fig. S3), likely due to the reduced

frequency of circulating autoreactive CD8$^+$ T cells in healthy subjects [48]. Therefore, to investigate the impact of DC$^{IL-10/Ag}$ on CD8$^+$ T cells, we used as model Ag the sequence encoding for Matrix Protein 1 (M1) of H1N1 influenza virus (Fig. S1). Engineered DC were generated from healthy subjects to obtain control DC (DC^{CLIP}) or M1-specific DC lacking or expressing hIL-10 (DC^{M1} and DC$^{IL-10/M1}$). DC^{CLIP}, DC^{M1} and DC$^{IL-10/M1}$ expressed similar levels of HLA class I, but DC$^{IL-10/M1}$ expressed significant higher levels of PD-L1 compared to control DC (Fig. S5A), demonstrating that over-expression of IL-10 led to the differentiation of tolDC able to present encoded Ags to CD8$^+$ T cells in the presence of inhibitory molecules. Like DC$^{IL-10/Ins}$, DC$^{IL-10/M1}$ displayed

a marked anti-inflammatory cytokine profile, with high levels of IL-10 and low production of IL-12/TNFα compared to control DC (Fig. S5B). DC^{M1} promoted expression of CD137, marker of Ag-specific activation CD8$^+$ T cell [49], in responder CD8$^+$ T cells, while DC$^{IL-10/M1}$ significantly reduced the frequency of M1-specific CD137$^+$ T cells (Fig. S4A). In line with decreased activation, we observed lower proliferation of M1-specific CD8$^+$ T cells compared to cultures stimulated with DC^{M1} (Fig. S4B) and a significant reduction in the frequency of IFNγ$^+$CD8$^+$ T cells in cultures obtained upon DC$^{IL-10/M1}$ (Fig. S4C). Inhibition of Ag-specific CD8$^+$ T cells was further confirmed by a strongly reduced release of IFNγ and TNFα in cell culture supernatants (Fig. S6A). DC$^{IL-10/M1}$ could efficiently prime CD8$^+$ T cells, as demonstrated by induction of CD71 expression on responder cells comparable to that elicited by DC^{M1} (Fig. S6B). Notably, addition of IL-10 during stimulation of CD8$^+$ T cells with DC^{M1} could not reproduce the consistent inhibition of Ag-specific CD8$^+$ T cell responses promoted by DC$^{IL-10/M1}$ (Fig. S6C). Thus, human DC engineered with LVs encoding for Ag and IL-10 are tolDC able to consistently downregulate Ag-specific CD8$^+$ T cell responses *in vitro*.

3.4. Human DC$^{IL-10/glia}$ inhibit pathogenic gliadin-specific CD4$^+$ T cells and promote gliadin-specific Tr1 cells in celiac disease patients

To test our tolerogenic engineered DC in a more disease-relevant setting, we modified the LV-Iip33-InsB$_{4-29}$ construct and subcloned a sequence comprising an epitope of alpha gliadin (deamidated α-gliadin 17-mer A-gliadin$_{57-73}$ Q65E, hereafter glia), the most active gluten peptide in HLA-DQ2$^+$ CD patients [50] (Fig. S1A). We generated DC by transducing PB CD14+ monocytes of CD patients (n = 17, Table 1) with LV-Iip33-CLIP, LV-Iip33-glia, or LV-IL-10/Iip33-glia to differentiate DC^{CLIP}, DC^{glia}, or DC$^{IL-10/glia}$, respectively. In most samples comparable DC yields and good transduction efficiencies of DC$^{IL-10/glia}$ were obtained (VCN>3 in 13/17) (Fig. S7A). Efficient transduction of DC$^{IL-10/glia}$ was confirmed by high levels of IL-10 production (Fig. S7A). DC$^{IL-10/glia}$ showed a significant higher expression of tolDC-associated markers CD141, CD163, CD14, CD16 and ILT4, compared to control DC (Fig. S7B). CD4$^+$ T cells after *in vitro* stimulation with autologous DC^{glia} proliferated and/or secreted IFNγ in a fraction of CD patients with (CD atrophic/CD-Atr) or without (CD potential/CD-Pot) damaged mucosa, but not in non-celiac subjects. Low levels of proliferation were observed with lymphocytes of CD patients on gluten-free-diet (CD-GFD) (Fig. 3A and B). The Ag-specific response of CD4$^+$ T cells from gliadin-responsive CD patients was inhibited when T cells were cultured with DC$^{IL-10/glia}$, thus confirming the ability of engineered DC to suppress the expansion of potentially pathogenic CD4$^+$ T cells (Fig. 3A).

Furthermore, stimulation of CD4$^+$ T cells from gliadin-responsive CD patients with autologous DC$^{IL-10/glia}$ for 10 days resulted in the generation of gliadin-specific T cells containing a significant higher frequency of CD49b+LAG-3$^+$ Tr1 cells (35.7 ± 8.1, mean ± SEM, n = 6) compared to that obtained in T cells stimulated with control DC^{glia} (12.4 ± 3.7, mean ± SEM, n = 6, Fig. 3C). Of note, Tr1 cells were not detected in T-DC$^{IL-10/glia}$ co-cultures of a CD patients who did not carry the HLA-DQ2 alleles (Fig. 3C).

These results demonstrate that DC$^{IL-10/Ag}$ derived from patients have the potential to control pathogenic T cell responses specific for the disease relevant Ag and promote the differentiation of Ag-specific Tr1 cells in HLA-DQ2$^+$ CD patients.

3.5. Generation and in vivo characterization of murine DC$^{IL-10/Ag}$

To demonstrate that DC$^{IL-10/Ag}$ can be applied to control Ag-specific immune response *in vivo*, we generated murine DC$^{IL-10/Ag}$. To this aim we subcloned LV constructs encoding for murine Ii fused to a specific Ag-derived peptide [34–36] alone or in combination with hIL-10 (LV-IL-10) [23,37]. Ags used in the present study include peptides from Ovalbumin (OVA), Insulin B-chain (InsB), and 2.5 Hybrid Insulin Peptide (2.5HIP) (Fig. S8A) [38]. Bone marrow (BM)-derived cells from C57Bl/6 and non-obese diabetic (NOD) mice were transduced during *in vitro* differentiation into DC with LVs encoding peptide-Ags alone (DC^{Ag}) or in combination with hIL-10 (DC$^{IL-10/Ag}$). As control, untransduced DC (DC^{UT}) were differentiated in parallel. DC$^{IL-10/Ag}$ showed significantly reduced expression levels of CD11c compared to DC^{UT} and DC^{Ag}, reduced expression of MHC class II and higher expression levels of PD-L1 on a per-cell base compared to DC^{Ag}, whereas CD80 and CD86 expression were comparable (Figs. S9A–B). Upon LPS-mediated activation, DC$^{IL-10/Ag}$ (mDC$^{IL-10/Ag}$), showed lower CD86 expression than mDC^{Ag}, whereas all other markers were comparable (Figs. S11A–B).

Characterization of cytokine production profile of DC$^{IL-10/Ag}$ at steady state and upon LPS stimulation showed that LV-mediated hIL-10 gene transfer into murine DC resulted in high levels of constitutive hIL-10 production (DC$^{IL-10/Ag}$ and LPS-DC$^{IL-10/Ag}$: 159.9 ± 5.5 and 164.3 ± 2.4 ng/ml, mean ± SEM, n = 7) (Fig. S9C). No major differences in murine (m)IL-10 secretion by DC$^{IL-10/Ag}$ and control DC were observed (Fig. S9C). Conversely, DC$^{IL-10/Ag}$ secreted significantly reduced levels of mIL-12p40 (p < 0,05, n = 5) and overall lower levels of mIL-12p70 (p = 0,06, n = 5, Fig. S9C) compared to control DC.

Overall, as demonstrated for human DC$^{IL-10/Ag}$, LV-mediated hIL-10 gene transfer in BM-derived DC drives the generation of DC with a pro-tolerogenic phenotype, the ability to secrete supra-physiological levels of hIL-10 and reduced amounts of the pro-inflammatory cytokine IL-12.

Table 1
Clinical and histological presentation of subjects investigated for celiac disease diagnosis enrolled in the study.

Pt	Diagnosis	Histology	Serology (TTG IgA, EMA)	HLA-DQ alleles (type)
GB006	CD-Atr	Marsh 3 b	>4965, +	DQA1*05$^+$DQB1*02$^+$ (HLA-DQ2.5)
GB012	CD-Atr	Marsh 3 b	176, +	DQA1*05$^+$DQB1*02$^-$DQB1*0301$^+$(HLA-DQ7)
GB018	CD-Atr	Marsh 3 b	220, +	DQA1*0201$^+$DQB1*02$^+$ (HLA-DQ2.2)
SAP07	CD-Atr	Marsh 3b/3c	99, +	DQA1*05$^+$DQB1*02$^+$ (HLA-DQ2.5)
SAP09	CD-Atr	Marsh 3c	126, +	DQA1*0201$^+$DQB1*02$^+$ (HLA-DQ2.2)
SAP12	CD-GFD	Marsh 0	-, n.t.	DQA1*05$^+$DQB1*02$^+$ (HLA-DQ2.5)
SAP13	CD-Pot	Marsh 1	67,6; +	DQA1*05$^+$DQB1*02$^+$ (HLA-DQ2.5)
SAP15	CD-Pot	Marsh 1	60, -	DQA1*0201$^+$DQB1*02$^+$ (HLA-DQ2.2)
SAP19	CD-Atr	Marsh 3a	48.1; +	DQA1*05$^+$DQB1*02$^+$ (HLA-DQ2.5)
SAP23	other	duodenitis	n.t.; n.t.	DQA1*05$^+$DQB1*02$^+$ (HLA-DQ2.5)
SAP31	other	unspecific	n.t.; weak+	DQA1*05$^+$DQB1*02$^+$ (HLA-DQ2.5)
SAP34	CD-Atr	Marsh 3 b	111.7; weak+	DQA1*05$^+$DQB1*02$^+$ (HLA-DQ2.5)
SAP39	CD-Pot	Marsh 0	-; -	DQA1*05$^+$DQB102$^-$DQB1*0301$^+$(HLA-DQ7)
SAP43	CD-Atr	Marsh 3b/3c	147; +	DQA1*05$^+$DQB1*02$^+$ (HLA-DQ2.5)
SAP47	CD-Atr	Marsh 3c	62; -	DQA1*05$^+$DQB1*02$^+$ (HLA-DQ2.5)
SAP57	other	Gastritis	-; -	DQA1*05$^+$DQB102$^-$ DQB1*0301$^+$(HLA-DQ7)
SAP58	CD-GFD	Marsh 2	n.t.; n.t.	DQA1*0201$^+$DQB1*02$^+$ (HLA-DQ2.2)

TTG: anti-transglutaminase autoantibodies; CD: celiac disease; Atr: atrophic; Pot: potential; EMA: anti-endomisium autoantibodies; GFD: gluten-free-diet; HLA: human leukocyte antigen; IgA: immunoglobulin A; n.t.: not tested; Pt: patient.

3.6. Murine DC$^{IL-10/Ag}$ modulate Ag-specific CD4$^+$ and CD8$^+$ T cell responses in vitro

Transduction of BM-derived DC with LV-IiAgs (OVA, HIP, or InsB) allowed encoded Ag presentation to CD4$^+$ T cells, leading to their activation and proliferation, which was higher than the responses elicited by control DC^{UT} (Fig. S10). Interestingly, stimulation of CD4$^+$ OTII cells with DC$^{IL-10/OVAs}$ (presenting OVA$_{323-339}$ peptide) induced activation of responder cells, evaluated based on cell surface CD25 expression [51]. DC$^{IL-10/OVAs}$-stimulated CD4$^+$ T cells showed a trend of reduced CD25 expression compared to T cells stimulated with DC^{OVAs} (Fig. 4A). Similar responses were observed when TCRtg CD4$^+$ BDC2.5 T

A

B

C
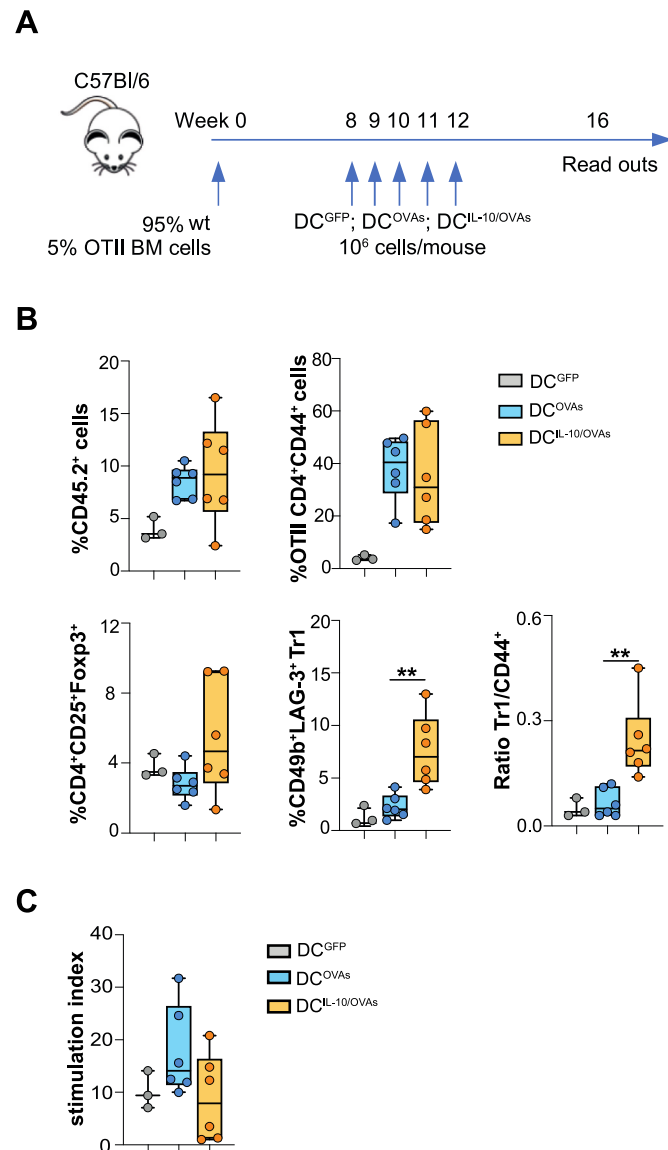
Fig. 4. DC$^{IL-10/OVA}$ induce OVA-specific Tr1 cells *in vivo*. (**A-D**) Experimental design for chimeric mice generation and DC treatment. (**B**) Percentages of CD45.2$^+$ cells, CD4$^+$CD44$^+$OTII T cells, CD25$^+$FOXP3$^+$ Tregs, CD49b$^+$LAG-3$^+$ Tr1, and ratio between Tr1/memory T cells in the spleen at end of experiment (EOE) are shown. (**C**) Splenic CD4$^+$ T were stimulated with DC^{OVAs} or DC^{UT}. Proliferation was measured by flow cytometry after 4 days. Data are reported as stimulation index (% divided T + DC^{OVAs}/% divided T + DC^{UT}). Results from immature DC^{GFP}- (n = 3), DC^{OVAs}- (n = 6), DC$^{IL-10/OVAs}$-(n = 6) treated mice from one experiment are shown. Box and whiskers (min to max) are presented. Dots represent single mice treated with DC. **: p < 0.01, Mann Whitney *U* test.

cells, expressing TCR specific for the T1D epitope 2.5HIP [38], that were stimulated with DC$^{IL-10/HIP}$, NOD CD4$^+$ T cells in response to DC transduced with InsB native peptide (DC$^{IL-10/InsB}$) or InsB mimetope (DC$^{IL-10/InsBR22E}$) and hIL-10 [52] (Fig. S10A).

Stimulation of CD8$^+$ OTI cells with DC^{OVAl} (expressing OVA$_{242-353}$ that contains the SIINFEKL peptide) efficiently (p < 0.01) promoted their activation (Fig. S10B). As observed for OTII CD4$^+$ T cells, stimulation of CD8$^+$ OTI cells with DC$^{IL-10/OVAl}$ induced an overall low CD25 expression on responder cells (p = ns, Fig. S10C). No Ag-specific activation was observed in NOD CD8$^+$ T cells stimulated with DC engineered with InsB-derived epitopes (Fig. S10C).

Regardless of the type of Ag presented, stimulation of CD4$^+$ T cells with DC$^{IL-10/Ag}$ always resulted in a significant lower proliferation as compared to that elicited by DC^{Ag}, which is most likely due to the high amounts of IL-10 produced (Fig. S10C). Similarly, the proliferative responses of OTI CD8$^+$ T cells to DC$^{IL-10/OVAl}$ were significantly inhibited compared to those elicited by DC^{OVAl} (Fig. S10D). While proliferation of NOD CD8$^+$ T cells in response to InsB native peptide was barely detectable, the few T cells proliferating to InsB mimetope were significantly inhibited by DC$^{IL-10/InsBR22E}$ (Fig. S10D). LPS-activated mDC$^{IL-10/Ag}$ only partially inhibited Ag-specific activation, as determined by CD25 expression of responder T cells (Figs. S11A–B), but significantly suppressed Ag-specific proliferation of both CD4$^+$ and CD8$^+$ T cells, compared to mDC^{Ag} (Figs. S12C–D).

Thus, murine IL-10/Ag-engineered DC efficiently inhibit activation and proliferation of Ag-specific CD4$^+$ and CD8$^+$ T cells and maintain their suppressive capacity following activation by pro-inflammatory stimuli.

3.7. Murine DC$^{IL-10/Ag}$ induce Ag-specific Tr1 cells in vivo

To investigate the mechanism of action of DC$^{IL-10/Ag}$ *in vivo*, we generated chimeric mice by transplanting C57BL/6 CD45.1 (95%) and CD45.2 OTII (5%) BM cells into lethally irradiated C57BL/6 CD45.1 recipients (Fig. 4A). At immune reconstitution, chimeric mice were repetitively injected with DC$^{IL-10/OVAs}$, DC^{OVAs} or DC^{GFP} (Fig. 4A). Administration of OVA-encoding DCs, but not DC^{GFP}, promoted the expansion of OTII cells with a memory phenotype (Fig. 4B), suggesting that OVA-specific T cell priming occurred *in vivo*. Despite their inhibitory effects on Ag-specific T cell activation and proliferation *in vitro*, administration of DC$^{IL-10/OVAs}$ surprisingly resulted in the induction of significantly higher numbers of OTII CD49b$^+$LAG-3$^+$ Tr1 cells and Tr1/ CD44$^+$ memory T cells (Fig. 4B). Interestingly, none of the DC treatments induced significant expansion of OVA-specific CD4$^+$CD25$^+$FOXP3$^+$ Tregs, likely due to the well-known function of IL-10 in the induction and maintenance of Tr1 cells [53,54] (Fig. 4B). Upon *in vitro* re-stimulation with DC^{OVAs}, splenic OVA-specific T cells isolated from DC$^{IL-10/OVAs}$-treated mice showed only a trend to reduced proliferation compared to those isolated from control DC^{OVAs}-treated mice, which is probably related to the presence of abundant residual naïve OTII cells in DC$^{IL-10/OVAs}$-treated mice (CD44$^-$, Fig. 4B) in the *in vitro* rechallenge (Fig. 4C).

Our results demonstrate that *in vivo* administration of DC$^{IL-10/Ag}$ modulates CD4$^+$ T cell responses by promoting the induction of Ag-specific Tr1 cells, but not FOXP3$^+$ Tregs.

3.8. In vivo administration of DC$^{IL-10/Ag}$ prevents type 1 diabetes development

To assess the efficacy of DC$^{IL-10/Ag}$ to induce functional Tr1 cells which prevent disease development, we used two distinct models of induced T1D: BDC2.5 T cell and NOD splenocyte transfer in immunodeficient recipients [55]. In the former, the adoptive transfer of diabetogenic CD4$^+$BDC2.5 T cells into NSG female recipients promoted T1D development in 14 days (Fig. 5A and B). Administration of DC^{HIP} to CD4$^+$BDC2.5 T cell-transferred mice accelerated T1D development
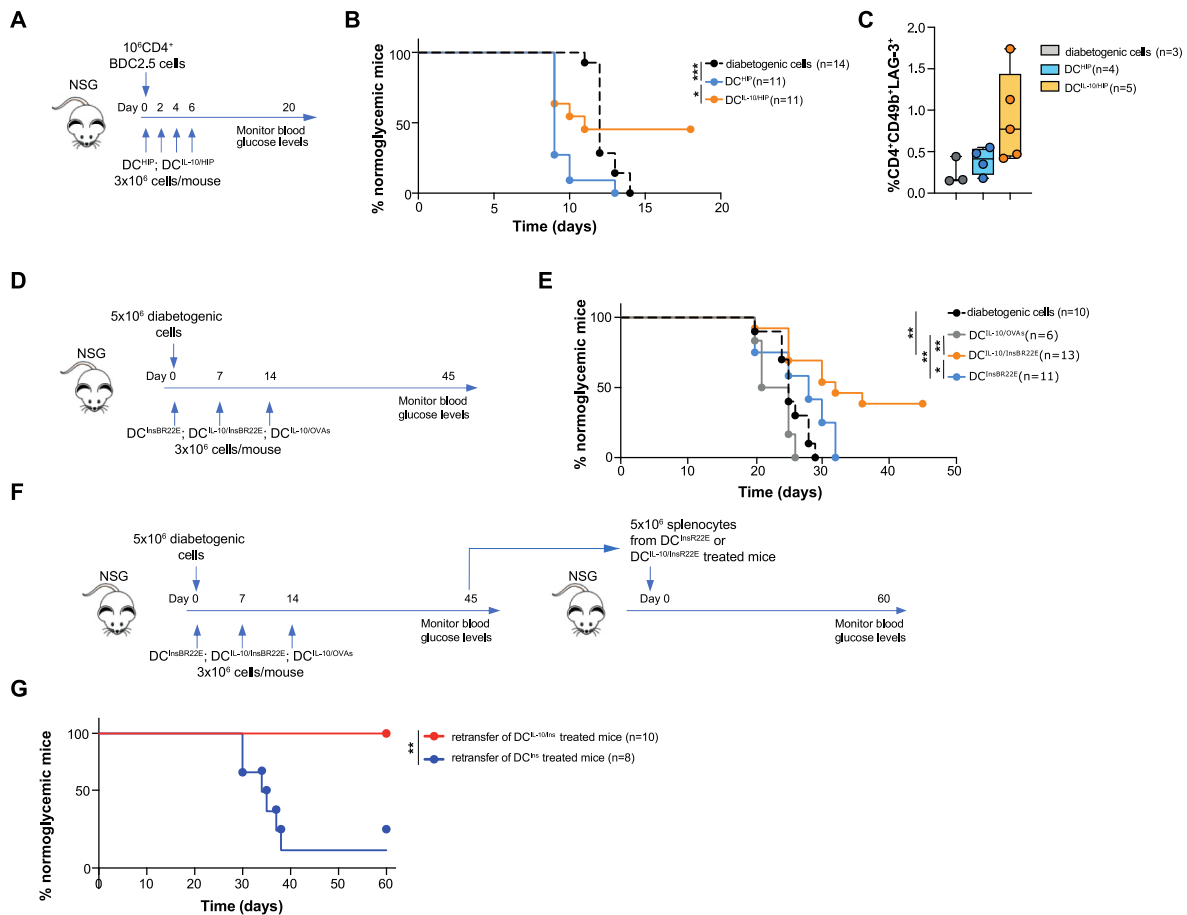
Fig. 5. $DC^{IL-10/HIP}$ and $DC^{IL-10/InsBR22E}$ *in vivo* administration prevents T1D development and induce long-term tolerance. (**A-D**) Experimental design for T1D induction in NSG mice upon transfer of diabetogenic cells and DC treatment. (**B**) Incidence of T1D in NSG recipients of TCRtg BDC2.5 T cells untreated (black, n = 14) or treated with DC^{HIP} (blue, n = 11) or $DC^{IL-10/HIP}$ (orange, n = 11). Results of three independent experiments were pooled. (**C**) Percentages of $CD4^+CD49b^+LAG-3^+$ T cells in the spleen of mice shown in (**B**) surviving up to day 18 are plotted in the graph. (**E**) Incidence of T1D in NSG recipients of diabetogenic NOD splenocytes untreated (black, n = 10) or treated with $DC^{InsBR22E}$ (blue, n = 11), $DC^{IL-10/InsBR22E}$ (orange, n = 13) or $DC^{IL-10/OVAs}$ (grey, n = 6). Results of two independent experiments were pooled. (**F**) Experimental design for T1D induction in NSG mice upon transfer of splenocytes from DC-treated mice. (**G**) Incidence of T1D in NSG recipients of splenocytes from mice treated with $DC^{InsBR22E}$ (blue, n = 8) or with $DC^{IL-10/InsBR22E}$ (red, n = 10). Results of two independent experiments were pooled. *: $p < 0.05$, **: $p < 0.01$, ***: $p < 0.001$, Log-rank (Mantel-Cox) test with Benjamini-Hochberg correction for multiple testing.

compared to mice receiving BDC2.5 cells alone ($p < 0.001$), while repetitive $DC^{IL-10/HIP}$ injections prevented diabetes development in 5 out of 11 treated mice (45% protection, $p < 0.05$ *vs* DC^{HIP}, Fig. 5B). In line with results described in the OTII model, administration of $DC^{IL-10/HIP}$ resulted in the induction of a higher frequency of $CD4^+CD49b^+ LAG-3^+$ T cells in the spleen, although analysis was feasible only in mice surviving up to the end of the experiment (Fig. 5C).

In the second model, adoptive transfer of splenocytes from diabetic NOD mice into NSG female recipients promoted T1D development in 28 days (Fig. 5D). Like the results obtained in BDC2.5 model, treatment with $DC^{IL-10/InsBR22E}$ prevented T1D development induced by diabetogenic T cells in 5 out of 13 treated mice (38% protection, $p < 0.05$ *vs* $DC^{InsBR22E}$; $p < 0.01$ *vs* control mice, Fig. 5E). Interestingly, injection of $DC^{IL-10/OVAs}$ did not prevent disease development (Fig. 5E), demonstrating that control of autoimmunity by $DC^{IL-10/Ag}$ requires the concomitant expression of IL-10 and presentation of disease-specific Ag to T cells. To confirm induction of long-term tolerance, at day 45 post-treatment, splenocytes isolated from diabetic $DC^{InsBR22E}$- or normoglycemic $DC^{IL-10/InsBR22E}$-treated mice were injected in new NSG recipients. None of the mice receiving cells from $DC^{IL-10/InsBR22E}$-treated mice developed diabetes ($p < 0,01$ *vs* $DC^{InsBR22E}$, Fig. 5F).

To assess whether $DC^{IL-10/Ag}$ administration could potentially interfere with protective immune response to pathogens, we tested *in vivo* response to LPS challenge, as model of sepsis-associated

dysregulated immune response, in the presence or absence of engineered DC (Fig. 6). Results indicate that administration of $DC^{IL-10/InBR22E}$ (3×10^6 cells/mouse) did not result in increased circulating human IL-10 in peripheral blood and did not impact on mice survival upon intraperitoneal injection of LPS (2.5 mg/kg), since all $DC^{IL-10/InBR22E}$-treated mice were alive up to 48 h after treatment (not shown). Response to sepsis was monitored by repeated measurement of inflammatory cytokines and chemokines (including TNFα, IL1β, IL-12, IL-10, MIP-1β and MCP-1) after LPS challenge (4-6-24 h). At the peak of innate response (4 h), cytokine levels were similar in treated mice or PBS controls, with only non-significant changes in TNFα and IL-12p70 levels at 6 h, which did not alter control of the acute inflammatory response at 24 h post LPS challenge, thus suggesting that the presence of $DC^{IL-10/InBR22E}$ did not significantly impact on host protection during sepsis in this model (Fig. 6).

Overall, these results demonstrate that *in vivo* $DC^{IL-10/Ag}$ administration is safe and controls autoimmune disease development in aggressive models of T1D and induce long-term tolerance, likely by induction of Ag-specific Tr1 cells.

4. Discussion

We developed a LV-based platform for the transduction of DC with both Ag-derived peptides and hIL-10. These *in vitro* generated Ag-

A

B
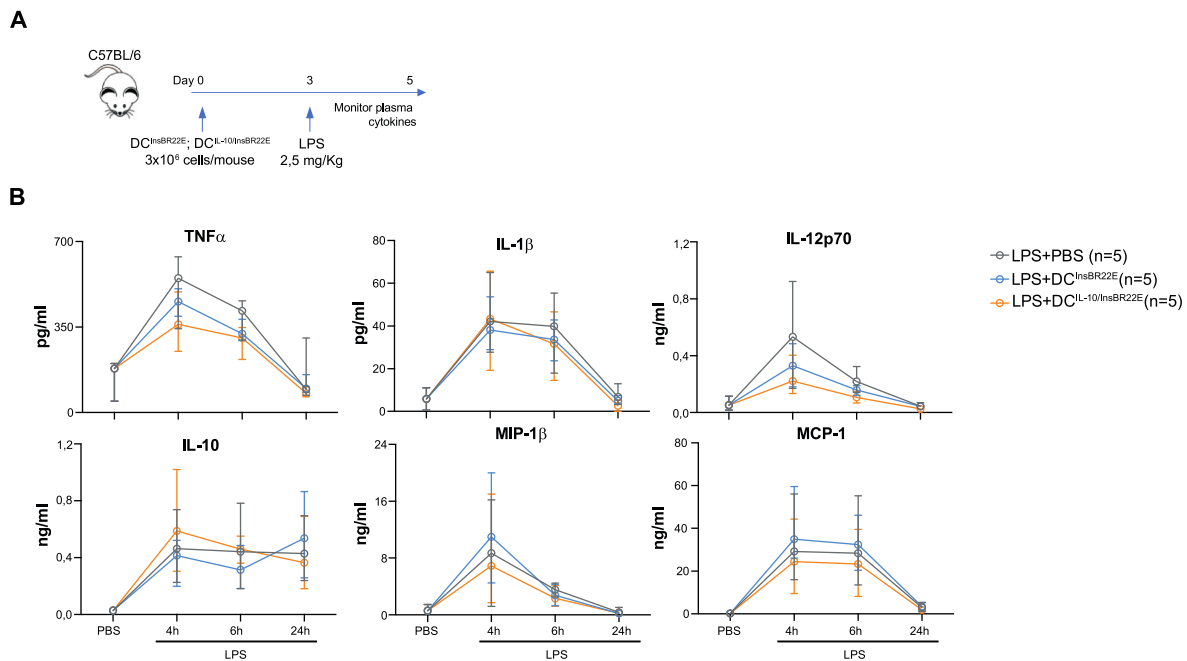
Fig. 6. $DC^{IL-10/Ag}$ do not alter *in vivo* response to LPS challenge

(**A**) Experimental design to induce and monitor acute inflammatory response to LPS challenge. (**B**) Concentration of TNFα, IL-1β, IL-12p70, IL-10, MIP-1β, and MCP-1 in sera at 4, 6 and 24 h after LPS challenge in mice pre-treated with $DC^{InsBR22E}$ (blue, n = 5), $DC^{IL-10/InsBR22E}$ (orange, n = 5), or PBS controls (grey, n = 5) was measured by Luminex assay. Median and range are presented; two-way ANOVA with Benjamini-Hochberg correction for multiple comparisons.

specific DC ($DC^{IL-10/Ag}$) display a semi-mature tolerogenic phenotype, secrete supra-physiological levels of hIL-10 and low amounts of pro-inflammatory cytokines. Human $DC^{IL-10/Ag}$ efficiently inhibit Ag-specific $CD4^+$ T cell responses and Ag-specific $CD8^+$ T cell functions in healthy subjects and promote the induction of *bona fide* Ag-specific Tr1 cells *in vitro*. $DC^{IL-10/Ag}$ modulate pathogenic gliadin-specific T cells from CD patients, showing efficient inhibition of pathogenic $CD4^+$ T cell functions and induction of gliadin-specific Tr1 *in vitro*. Notably, murine $DC^{IL-10/Ag}$ also inhibit $CD4^+$ and $CD8^+$ T cell effector functions *in vitro* and administration of murine $DC^{IL-10/Ag}$ confirmed the induction of Ag-specific Tr1 cells *in vivo*. More importantly, administration of $DC^{IL-10/diabetogenic\ peptide}$ prevented disease development in 38% and 45% of recipients in two aggressive preclinical T1D models through the induction of Ag-specific Tr1 cells, which upon subsequent transfer completely prevented T1D.

Previous studies have consistently shown that fusion of Ag-encoding sequences to Ii increases T cell responses to the encoded transgene, due to favorable processing and presentation in the context of MHC class I and targeting of transgenic peptides for MHC class II loading [32–35]. In the present study we applied for the first time the same approach in human and murine DC, to induce Ag-specific tolerance through a tolDC-based strategy. Our results demonstrate the versatility of the platform, here applied to model (OVA), self (InsB), dietary (glia) and diabetogenic (HIP, InsBR22E) Ags, and consistently sustain the ability of Ag/IL-10-engineered tolDC to downregulate Ag-specific $CD4^+$ T cell responses, a key issue for the success of tol-DC based therapies. Indeed, in experimental autoimmune encephalomyelitis (EAE) mice a beneficial effect of tolDC therapy was only observed when VitD3-tolDC were pulsed with the adequate immunogenic peptide [56,57]. Since Ii-Ag transduction ensures a continuous source of Ag for presentation to T cells, the engineered tolDC product displays increased efficiency of Ag-presentation over previously tested Ag-pulsing based strategies.

The crucial role of IL-10 in the modulation of human Ag-presenting cells and the differentiation of Tr1 cells has been widely demonstrated in the past [11,25,58,59]. Here we confirm that IL-10-conditioned DC precursors differentiate *in vitro* into potent tolDC, as previously reported for IL-10-modulated DC (DC-10) [11] or LV-IL-10 engineered DC

(DC^{IL-10}) [25]. Although *in vitro* results from human PB were affected by the overall low frequency of circulating autoAg-specific T cells in healthy subjects and CD patients, we could detect both consistent inhibition of Ag-specific $CD4^+$ T effector functions and induction of *bona fide* Tr1 cells, as demonstrated by a transcriptional profile super-imposable to that of well-defined Tr1 cell products [40,43]. Importantly, we show that multiple administrations of $DC^{IL-10/Ag}$ allow selective expansion of Ag-specific Tr1 cells, showing that $DC^{IL-10/Ag}$ *in vivo* activity is not limited to the inhibition of Ag-specific T effector cells. These finding indicate a unique property of $DC^{IL-10/Ag}$ over previously tested tolDC-based approaches, which have consistently demonstrated induction of human T $CD4^+$ cell hypo-responsiveness, without clear evidence of Ag-specific Treg cell induction [19,60], with the exception of mild changes in the frequency of $FOXP3^+$ Tregs [14,21,61] and IL-10-producing $CD4^+$ T cells [20] in few trials. We are aware that *in vivo* induction of Tr1 cells was not consistently demonstrated in the T1D pre clinical models here presented, since the short-time of observation and disease severity in the BDC2.5 T1D model allowed analysis esclusively in a fraction of treated mice and technical limitations did not allow detection of Ins-specific T cells in NSG-transferred mice. Nonetheless, results of secondary transfer demonstrate that $DC^{IL-10/Ag}$ establish long-term active tolerance, which is stably maintained long after *in vivo* DC survival, estimated to be not longer than 10 days [25]. Based on these results, we propose that *in vivo* administration of $DC^{IL-10/Ag}$ not only controls T effector cell responses *in vitro* and T effector cell mediated tissue damage *in vivo*, but also initiates an Ag-specific self-sustaining tolerogenic loop, likely mediated by long-term Ag-specific Tr1 cells. Therefore, our platform represents a step forward in tolDC-based approaches since IL-10-engineered DC better target pathogenic responses and promote long-term tolerance due to their unique ability to induce Ag-specific Tr1 cells.

Moreover, we demonstrate that $DC^{IL-10/Ag}$ efficiently control $CD8^+$ T effector functions against model Ags in both humans and mice. Autoreactive $CD8^+$ T cells play a fundamental role in several autoimmune diseases [62]. In NOD mice, $CD8^+$ T effector cells are key players in the destruction of pancreatic β-cells and contribute to sustain islet inflammation [63,64]. On the other hand, in T1D patients the presence of

exhausted CD8$^+$ T cells is associated with slow disease progression [65] and better response to teplizumab therapy [66]. Therefore, efficient control of the CD8$^+$ T effector compartment is critical in therapeutic interventions in diseases such as T1D. In the NOD splenocytes transfer model, DC$^{IL-10/Ins}$ could control T1D onset in the presence of diabetogenic CD8$^+$ T cells, thus supporting the idea that persistent Ag-stimulation concomitant to IL-10 supplementation enhances CD8$^+$ T cell dysfunction [67]. Blockade of Ag-specific pathogenic CD8$^+$ T effector cells represents a key advantage of the DC$^{IL-10/Ag}$ platform, not previously reported for DC-based cell therapy [14,19–21,61,68].

5. Conclusions

Overall, our results indicate that DC$^{IL-10/Ag}$ are superior to previously described tolDC-based approaches used to restore tolerance because they have the capacity, not only to directly down regulate pathogenic CD4$^+$ and CD8$^+$ effector T cell responses, but also to induce Ag-specific Tr1 cells. The DC$^{IL-10/Ag}$ product could be used as a platform to induce single or multiple Ag-specific tolerance in autoimmune and other T cell mediated disease with high unmet medical need.

Author statement

We confirm that the manuscript has been read and approved by all named authors and that there are no other persons who satisfied the criteria for authorship but are not listed. We further confirm that the order of authors listed in the manuscript has been approved by all of us.

Funding

Author statement

SG, AA, and LPasserini conceptualized the study, designed experiments, and supervised the study. LPasseri, IM, FR and CL performed *in vivo* and *in vitro* experiments with murine samples. LC produced LVs. GA, LPasserini, VB, SV performed experiments with human samples. GG performed bioinformatic analyses. LPasserini, LPasseri and GA analyzed data. PS, GB, LF, RA, RT, GDN, CZ and MDS collected biological samples and managed CD patients' database. LPasseri and LPasserini wrote the manuscript that was reviewed by SG and AA. PS, GB, LF, CG, RT, RA, GDN participated in data discussion and interpretation of results. All authors have read and approved the final manuscript for submission.

Declaration of competing interest

None.

Data availability

Data will be made available on request.

Acknowledgements

Appendix A. Supplementary data

Supplementary data to this article can be found online at https://doi.org/10.1016/j.jaut.2023.103051.

References

[1] M.F. Huffaker, S. Sanda, S. Chandran, S.A. Chung, E.W. St Clair, G.T. Nepom, et al., Approaches to establishing tolerance in immune mediated diseases, Front. Immunol. 12 (2021), 744804.

[2] G.S. Cooper, M.L. Bynum, E.C. Somers, Recent insights in the epidemiology of autoimmune diseases: improved prevalence estimates and understanding of clustering of diseases, J. Autoimmun. 33 (2009) 197–207.

[3] A. Cardo, I. Churruca, A. Lasa, V. Navarro, M. Vazquez-Polo, G. Perez-Junkera, et al., Nutritional mmbalances in ldult celiac patients following a gluten-free diet, Nutrients 13 (2021).

[4] D.E. Smilek, M.R. Ehlers, G.T. Nepom, Restoring the balance: immunotherapeutic combinations for autoimmune disease, Dis Model Mech 7 (2014) 503–513.

[5] G. Blanchard-Rohner, Vaccination in Children with autoimmune pisorders and treated with various immunosuppressive Regimens: a Comprehensive review and practical suide, Front. Immunol. 12 (2021), 711637.

[6] L.C. Cappelli, A.A. Shah, The relationships between cancer and autoimmune rheumatic diseases, Best Pract. Res. Clin. Rheumatol. 34 (2020), 101472.

[7] M. Fortunato, K. Morali, L. Passeri, S. Gregori, Regulatory cell therapy in organ transplantation: bchievements and open iuestions, Front. Immunol. 12 (2021), 641596.

[8] C. Ohnmacht, A. Pullner, S.B. King, I. Drexler, S. Meier, T. Brocker, et al., Constitutive ablation of dendritic cells breaks self-tolerance of CD4 T cells and results in spontaneous fatal autoimmunity, J. Exp. Med. 206 (2009) 549–559.

[9] M. Colonna, F. Navarro, T. Bellon, M. Llano, P. Garcia, J. Samaridis, et al., A common inhibitory receptor for major histocompatibility complex class I molecules on human lymphoid and myelomonocytic cells, J. Exp. Med. 186 (1997) 1809–1818.

[10] N.A. Fanger, C.R. Maliszewski, K. Schooley, T.S. Griffith, Human dendritic cells mediate cellular apoptosis via tumor necrosis factor-related apoptosis-inducing ligand (TRAIL), J. Exp. Med. 190 (1999) 1155–1164.

[11] S. Gregori, D. Tomasoni, V. Paccani, M. Scirpoli, M. Battaglia, C.F. Magnani, et al., Differentiation of type 1 T regulatory cells (Tr1) by tolerogenic DC-10 requires the IL-10-dependent ILT4/HLA-G pathway, Blood 116 (2010) 935–944.

[12] C.C. Chu, N. Ali, P. Karagiannis, P. Di Meglio, A. Skowera, L. Napolitano, et al., Resident CD141 (BDCA3)+ dendritic cells in human skin produce IL-10 and induce regulatory T cells that suppress skin inflammation, J. Exp. Med. 209 (2012) 935–945.

[13] B. Willekens, I. Wens, K. Kouters, P. Cras, N. Cools, Safety and immunological proof-of-concept following treatment with tolerance-inducing cell products in patients with autoimmune diseases or receiving organ transplantation: a systematic review and meta-analysis of clinical trials, Autoimmun. Rev. 20 (2021), 102873.

[14] N. Giannoukakis, B. Phillips, D. Finegold, J. Harnaha, M. Trucco, Phase I (safety) study of autologous tolerogenic dendritic cells in type 1 diabetic patients, Diabetes Care 34 (2011) 2026–2032.

[15] L. Piemonti, P. Monti, P. Allavena, M. Sironi, L. Soldini, B.E. Leone, et al., Glucocorticoids affect human dendritic cell differentiation and maturation, J. Immunol. 162 (1999) 6473–6481.

[16] G.B. Ferreira, A.S. Vanherwegen, G. Eelen, A.C.F. Gutierrez, L. Van Lommel, K. Marchal, et al., Vitamin D3 induces tolerance in human dendritic cells by activation of cntracellular setabolic pathways, Cell Rep. 10 (2015) 711–725.

[17] T. Taner, H. Hackstein, Z. Wang, A.E. Morelli, A.W. Thomson, Rapamycin-treated, alloantigen-pulsed host dendritic cells induce ag-specific T cell regulation and prolong graft survival, Am. J. Transplant. 5 (2005) 228–236.

[18] E. Marin, L. Bouchet-Delbos, O. Renoult, C. Louvet, V. Nerriere-Daguin, A. J. Managh, et al., Human tolerogenic dendritic cells regulate immune responses through eactate Synthesis, Cell Metabol. 30 (2019) 1075–10790 e8.

[19] G.M. Bell, A.E. Anderson, J. Diboll, R. Reece, O. Eltherington, R.A. Harry, et al., Autologous tolerogenic dendritic cells for rheumatoid and inflammatory arthritis, Ann. Rheum. Dis. 76 (2017) 227–234.

[20] I. Zubizarreta, G. Florez-Grau, G. Vila, R. Cabezon, C. Espana, M. Andorra, et al., Immune tolerance in multiple sclerosis and neuromyelitis optica with peptide-loaded tolerogenic dendritic cells in a phase 1b trial, Proc. Natl. Acad. Sci. U. S. A. 116 (2019) 8463–8470.

[21] H. Benham, H.J. Nel, S.C. Law, A.M. Mehdi, S. Street, N. Ramnoruth, et al., Citrullinated peptide dendritic cell immunotherapy in HLA risk genotype-positive rheumatoid arthritis patients, Sci. Transl. Med. 7 (2015) 290ra87.

[22] A. Follenzi, L.E. Ailles, S. Bakovic, M. Geuna, L. Naldini, Gene transfer by lentiviral vectors is limited by nuclear translocation and rescued by HIV-1 pol sequences, Nat. Genet. 25 (2000) 217–222.

[23] M. Amendola, M.A. Venneri, A. Biffi, E. Vigna, L. Naldini, Coordinate dual-gene transgenesis by lentiviral vectors carrying synthetic bidirectional promoters, Nat. Biotechnol. 23 (2005) 108–116.

[24] J.A. Medin, M. Migita, R. Pawliuk, S. Jacobson, S. Amiri, S. Kluepfel-Stahl, et al., A bicistronic therapeutic retroviral vector enables sorting of transduced CD34+

cells and corrects the enzyme deficiency in cells from Gaucher patients, Blood 87 (1996) 1754–1762.

[25] M. Comi, G. Amodio, L. Passeri, M. Fortunato, F.R. Santoni de Sio, G. Andolfi, et al., Generation of howerful human tolerogenic dendritic cells by lentiviral-mediated IL-10 gene transfer, Front. Immunol. 11 (2020) 1260.

[26] A. Dobin, C.A. Davis, F. Schlesinger, J. Drenkow, C. Zaleski, S. Jha, et al., STAR: ultrafast universal RNA-seq aligner, Bioinformatics 29 (2013) 15–21.

[27] Y. Liao, G.K. Smyth, W. Shi featureCounts, An efficient general purpose program for assigning sequence reads to genomic features, Bioinformatics 30 (2014) 923–930.

[28] M.I. Love, W. Huber, S. Anders, Moderated estimation of fold change and dispersion for RNA-seq data with DESeq2, Genome Biol. 15 (2014) 550.

[29] A. Subramanian, P. Tamayo, V.K. Mootha, S. Mukherjee, B.L. Ebert, M.A. Gillette, et al., Gene set enrichment analysis: a knowledge-based approach for interpreting genome-wide expression profiles, Proc. Natl. Acad. Sci. U. S. A. 102 (2005) 15545–15550.

[30] Z. Gu, R. Eils, M. Schlesner, Complex heatmaps reveal patterns and correlations in multidimensional genomic data, Bioinformatics 32 (2016) 2847–2849.

[31] S. Copeland, H.S. Warren, S.F. Lowry, S.E. Calvano, D. Remick, Inflammation et al. Acute inflammatory response to endotoxin in mice and humans, Clin. Diagn. Lab. Immunol. 12 (2005) 60–67.

[32] N. Mensali, A. Grenov, N.B. Pati, P. Dillard, M.R. Myhre, G. Gaudernack, et al., Antigen-delivery through invariant chain (CD74) boosts CD8 and CD4 T cell immunity, OncoImmunology 8 (2019), 1558663.

[33] I. Esposito, P. Cicconi, A.M. D'Alise, A. Brown, M. Esposito, L. Swadling, et al., MHC class II invariant chain-adjuvanted viral vectored vaccines enhances T cell responses in humans, Sci. Transl. Med. 12 (2020).

[34] S.S. Diebold, M. Cotten, N. Koch, M. Zenke, MHC class II presentation of endogenously expressed antigens by transfected dendritic cells, Gene Ther. 8 (2001) 487–493.

[35] H.M. Rowe, L. Lopes, Y. Ikeda, R. Bailey, I. Barde, M. Zenke, et al., Immunization with a lentiviral vector stimulates both CD4 and CD8 T cell responses to an ovalbumin transgene, Mol. Ther. 13 (2006) 310–319.

[36] F. Arce, H.M. Rowe, B. Chain, L. Lopes, M.K. Collins, Lentiviral vectors transduce proliferating dendritic cell precursors leading to persistent antigen presentation and immunization, Mol. Ther. 17 (2009) 1643–1650.

[37] G. Andolfi, G. Fousteri, M. Rossetti, C.F. Magnani, T. Jofra, G. Locafaro, et al., Enforced IL-10 expression confers type 1 regulatory T cell (Tr1) phenotype and function to human CD4(+) T cells, Mol. Ther. 20 (2012) 1778–1790.

[38] T. Delong, T.A. Wiles, R.L. Baker, B. Bradley, G. Barbour, R. Reisdorph, et al., Pathogenic CD4 T cells in type 1 diabetes recognize epitopes formed by peptide fusion, Science 351 (2016) 711–714.

[39] M. Comi, D. Avancini, F. Santoni de Sio, M. Villa, M.J. Uyeda, M. Floris, et al., Coexpression of CD163 and CD141 identifies human circulating IL-10-producing dendritic cells (DC-10), Cell. Mol. Immunol. 17 (2020) 95–107.

[40] N. Gagliani, C.F. Magnani, S. Huber, M.E. Gianolini, M. Pala, P. Licona-Limon, et al., Coexpression of CD49b and LAG-3 identifies human and mouse T regulatory type 1 cells, Nat. Med. 19 (2013) 739–746.

[41] L.G. Hidalgo, G. Einecke, K. Allanach, P.F. Halloran, The transcriptome of human cytotoxic T cells: similarities and disparities among allostimulated CD4(+) CTL, CD8(+) CTL and NK cells, Am. J. Transplant. 8 (2008) 627–636.

[42] J.S. Alfen, P. Larghi, F. Facciotti, N. Gagliani, R. Bosotti, M. Paroni, et al., Intestinal IFN-gamma-producing type 1 regulatory T cells coexpress CCR5 and programmed cell death protein 1 and downregulate IL-10 in the inflamed guts of patients with inflammatory bowel disease, J. Allergy Clin. Immunol. 142 (2018) 1537–15347 e8.

[43] P.P. Chen, A.M. Cepika, R. Agarwal-Hashmi, G. Saini, M.J. Uyeda, D.M. Louis, et al., Alloantigen-specific type 1 regulatory T cells suppress through CTLA-4 and PD-1 pathways and persist long-term in patients, Sci. Transl. Med. 13 (2021), eabf5264.

[44] A.M. Pesenacker, A.Y. Wang, A. Singh, J. Gillies, Y. Kim, C.A. Piccirillo, et al., A regulatory T-cell gene signature is a specific and Sensitive eiomarker to Identify Children with new-onset type 1 diabetes, Diabetes 65 (2016) 1031–1039.

[45] E. Martinuzzi, G. Novelli, M. Scotto, P. Blancou, J.M. Bach, L. Chaillous, et al., The frequency and immunodominance of islet-specific CD8+ T-cell responses change after type 1 diabetes diagnosis and treatment, Diabetes 57 (2008) 1312–1320.

[46] A.M. Anderson, L.G. Landry, A.A. Alkanani, L. Pyle, A.C. Powers, M.A. Atkinson, et al., Human islet T cells are highly reactive to preproinsulin in type 1 diabetes, Proc. Natl. Acad. Sci. U. S. A. (2021) 118.

[47] H.A. Abdelsamed, C.C. Zebley, H. Nguyen, R.L. Rutishauser, Y. Fan, H.E. Ghoneim, et al., Beta cell-specific CD8(+) T cells maintain stem cell memory-associated epigenetic programs during type 1 diabetes, Nat. Immunol. 21 (2020) 578–587.

[48] K.Y. Ma, A.A. Schonnesen, C. He, A.Y. Xia, E. Sun, E. Chen, et al., High-throughput and high-dimensional single-cell analysis of antigen-specific CD8(+) T cells, Nat. Immunol. 22 (2021) 1590–1598.

[49] M. Wolfl, J. Kuball, W.Y. Ho, H. Nguyen, T.J. Manley, M. Bleakley, et al., Activation-induced expression of CD137 permits detection, isolation, and expansion of the full repertoire of CD8+ T cells responding to antigen without requiring knowledge of epitope specificities, Blood 110 (2007) 201–210.

[50] A. Camarca, R.P. Anderson, G. Mamone, O. Fierro, A. Facchiano, S. Costantini, et al., Intestinal T cell responses to gluten peptides are largely heterogeneous: implications for a peptide-based therapy in celiac disease, J. Immunol. 182 (2009) 4158–4166.

[51] F. Fuhrmann, T. Lischke, F. Gross, T. Scheel, L. Bauer, K.W. Kalim, et al., Adequate immune response ensured by binary IL-2 and graded CD25 expression in a murine transfer model, Elife 5 (2016).

[52] C. Daniel, B. Weigmann, R. Bronson, H. von Boehmer, Prevention of type 1 diabetes in mice by tolerogenic vaccination with a strong agonist insulin mimetope, J. Exp. Med. 208 (2011) 1501–1510.

[53] L. Brockmann, N. Gagliani, B. Steglich, A.D. Giannou, J. Kempski, P. Pelczar, et al., IL-10 receptor Signaling is Essential for TR1 cell function in vivo, J. Immunol. 198 (2017) 1130–1141.

[54] H. Groux, A. O'Garra, M. Bigler, M. Rouleau, S. Antonenko, J.E. de Vries, et al., A CD4+ T-cell subset inhibits antigen-specific T-cell responses and prevents colitis, Nature 389 (1997) 737–742.

[55] T.L. Van Belle, P. Taylor, M.G. von Herrath, Mouse models for type 1 diabetes, Drug Discov. Today Dis. Model. 6 (2009) 41–45.

[56] M.J. Mansilla, R. Contreras-Cardone, J. Navarro-Barriuso, N. Cools, Z. Berneman, C. Ramo-Tello, et al., Cryopreserved vitamin D3-tolerogenic dendritic cells pulsed with autoantigens as a potential therapy for multiple sclerosis patients, J. Neuroinflammation 13 (2016) 113.

[57] M.J. Mansilla, C. Selles-Moreno, S. Fabregas-Puig, J. Amoedo, J. Navarro-Barriuso, A. Teniente-Serra, et al., Beneficial effect of tolerogenic dendritic cells pulsed with MOG autoantigen in experimental autoimmune encephalomyelitis, CNS Neurosci. Ther. 21 (2015) 222–230.

[58] K. Steinbrink, M. Wolfl, H. Jonuleit, J. Knop, A.H. Enk, Induction of tolerance by IL-10-treated dendritic cells, J. Immunol. 159 (1997) 4772–4780.

[59] M. Hubo, B. Trinschek, F. Kryczanowsky, A. Tuettenberg, K. Steinbrink, H. Jonuleit, Costimulatory molecules on immunogenic versus tolerogenic human dendritic cells, Front. Immunol. 4 (2013) 82.

[60] J. Navarro-Barriuso, M.J. Mansilla, B. Quirant-Sanchez, A. Teniente-Serra, C. Ramo-Tello, E.M. Martinez-Caceres, Vitamin D3-induced tolerogenic dendritic cells modulate the Transcriptomic profile of T CD4(+) cells towards a functional Hyporesponsiveness, Front. Immunol. 11 (2020), 599623.

[61] A. Jauregui-Amezaga, R. Cabezon, A. Ramirez-Morros, C. Espana, J. Rimola, C. Bru, et al., Intraperitoneal administration of autologous tolerogenic dendritic cells for Refractory Crohn's disease: a phase I study, J Crohns Colitis 9 (2015) 1071–1078.

[62] Q. Deng, Y. Luo, C. Chang, H. Wu, Y. Ding, R. Xiao, The Emerging epigenetic role of CD8+T cells in autoimmune diseases: a systematic review, Front. Immunol. 10 (2019) 856.

[63] M.S. Anderson, J.A. Bluestone, The NOD mouse: a model of immune dysregulation, Annu. Rev. Immunol. 23 (2005) 447–485.

[64] A.E. Wiedeman, C. Speake, S.A. Long, The many faces of islet antigen-specific CD8 T cells: clues to clinical outcome in type 1 diabetes, Immunol. Cell Biol. 99 (2021) 475–485.

[65] A.E. Wiedeman, V.S. Muir, M.G. Rosasco, H.A. DeBerg, S. Presnell, B. Haas, et al., Autoreactive CD8+ T cell exhaustion distinguishes subjects with slow type 1 diabetes progression, J. Clin. Invest. 130 (2020) 480–490.

[66] S.A. Long, J. Thorpe, H.A. DeBerg, V. Gersuk, J. Eddy, K.M. Harris, et al., Partial exhaustion of CD8 T cells and clinical response to teplizumab in new-onset type 1 diabetes, Sci Immunol (2016) 1.

[67] P.S. Linsley, S.A. Long, Enforcing the checkpoints: harnessing T-cell exhaustion for therapy of T1D, Curr. Opin. Endocrinol. Diabetes Obes. 26 (2019) 213–218.

[68] T. Nikolic, J.J. Zwaginga, B.S. Uitbeijerse, N.J. Woittiez, E.J. de Koning, H. J. Aanstoot, et al., Safety and feasibility of intradermal injection with tolerogenic dendritic cells pulsed with proinsulin peptide-for type 1 diabetes, Lancet Diabetes Endocrinol. 8 (2020) 470–472.